



Effect of heat treatment on the morphology, diameter and mesoporous of superfine glass fiber

Feiyan Wang , Jianyong Yu , Xunmei Liang , Shide Lu , Zhaolin Liu & Lifang Liu

To cite this article: Feiyan Wang , Jianyong Yu , Xunmei Liang , Shide Lu , Zhaolin Liu & Lifang Liu (2020): Effect of heat treatment on the morphology, diameter and mesoporous of superfine glass fiber, The Journal of The Textile Institute, DOI: [10.1080/00405000.2020.1798614](https://doi.org/10.1080/00405000.2020.1798614)

To link to this article: <https://doi.org/10.1080/00405000.2020.1798614>



© 2020 The Author(s). Published by Informa UK Limited, trading as Taylor & Francis Group.



Published online: 28 Jul 2020.



Submit your article to this journal [↗](#)



Article views: 135



View related articles [↗](#)



View Crossmark data [↗](#)

Effect of heat treatment on the morphology, diameter and mesoporous of superfine glass fiber

Feiyang Wang^{a,b}, Jianyong Yu^c, Xunmei Liang^d, Shide Lu^d, Zhaolin Liu^e and Lifang Liu^{a,c}

^aCollege of Textiles, Donghua University, Shanghai, PR China; ^bSchool of Textile and Clothing, Nantong University, Nantong, Jiangsu, PR China; ^cInnovation Center for Textile Science and Technology, Donghua University, Shanghai, PR China; ^dTaian Road Engineering Materials Co., Ltd, Taian, Shandong, PR China; ^eCollege of Textile and Garment, Hebei University of Science and Technology, Shijiazhuang, Hebei, PR China

ABSTRACT

Superfine glass fibers have high-temperature resistance, but they are rarely used and investigated at high temperature. In this article, the morphology, diameter and mesoporous are investigated by treating the superfine glass fiber felt during 400–650 °C. The result shows that the surface of heated fiber is smoother than original one; the diameter increases at 400 °C, then decreases with the increasing temperature, finally decreases by 14% at 600 °C; the mean mesoporous size increases with the increasing temperature, except at 500 °C, it increases 5.13 times at 600 °C. During heat treatment, the sizing agents gradually melt, decompose, and finally accumulate in very tinier areas on the surface of fiber; however, inside the fiber, the residual stress is released, the carbonate decomposes and melts. The released residual stress contributes to the increase of diameter, while thermal decomposition and thermal contraction cause the diameter to decrease and the mesoporous size to increase. The fiber stays in a metastable state, and has weight gain phenomenon when heated during 400–550 °C, while in a stable state at 600 °C, finally are destroyed at 650 °C.

ARTICLE HISTORY

Received 26 June 2019
Accepted 6 January 2020

KEYWORDS

Superfine glass fiber; heat treatment; mesoporous; weight gain phenomenon; topography

1. Introduction

Glass fiber is an inorganic nonmetallic material with good chemical stability, good thermal insulation, strong heat resistance and high mechanical strength. Normally, it is used as reinforcement in compound materials to improve the stiffness, strength and other properties (Bal et al., 2015; Sever et al., 2008). Most of researches focused on the influence of glass fiber on the comprehensive properties of compound materials (H. Chen et al., 2018; Elbadry et al., 2017; Raju et al., 2013), and the interfacial strength of the glass fiber-reinforced composites (Minty et al., 2018). The properties of glass fibers itself have also been investigated (Gao et al., 2007).

Some researchers paid attention to the performance of glass fiber reinforced composites at different temperatures. For example, the bonded strengths of glass fiber reinforced materials were investigated under a range of different temperatures (0–250 °C) (Abbasi & Hogg, 2005; Katz & Berman, 2000); the residual behavior of E-CR glass fiber reinforced polymer bars were researched under high-temperature treatment, ranging between 100 and 700 °C (Spagnuolo et al., 2018.); the influence of diffusion temperature on the water uptake and subsequent degradation behavior of multi-walled carbon nanotube embedded in glass fiber/epoxy composites was elucidated under the temperatures of 25 °C and 90 °C,

respectively (Prusty et al., 2018). For glass fiber itself, the strength degradation of the bundles of E-glass fiber and Advantex glass fibers were investigated under high temperatures up to 650 °C (Feih et al., 2009); the tensile mechanical behavior of AR-glass filament yarn was researched under the temperatures of 100–700 °C (Younes et al., 2014); the thermal stability, thermo-mechanical and mechanical properties of glass fiber rovings were improved at the temperature of 20–400 °C by polysilazane based thermal resistant coating treatment (Shayed et al., 2010.). Those researches focused on the mechanical properties of glass fiber at high temperature, as well as the method of improving its thermal mechanical properties, however ignored the performance of glass fiber itself at high temperature. Hence, it is important to reveal the change of interior structure and heat-treated mechanism of glass fiber itself under high temperature.

There are many kinds of glass fibers, which in general, can be classified by the compositions of glass raw materials, monofilament diameter, fiber appearance, production methods and fiber properties. Normally, the diameter of glass fiber less than 10 μm is defined as superfine glass fiber. By compared with normal glass fiber, the superfine glass fiber owns smaller diameter, lighter mass, better flexibility and lower cost of preparation. Most of them are used in normal temperature environment (Z. F. Chen et al., 2016; Wang

CONTACT Lifang Liu  lifangliu@dhu.edu.cn; Zhaolin Liu  liuzhaolin0508@163.com

© 2020 The Author(s). Published by Informa UK Limited, trading as Taylor & Francis Group.
This is an Open Access article distributed under the terms of the Creative Commons Attribution-NonCommercial-NoDerivatives License (<http://creativecommons.org/licenses/by-nc-nd/4.0/>), which permits non-commercial re-use, distribution, and reproduction in any medium, provided the original work is properly cited, and is not altered, transformed, or built upon in any way.

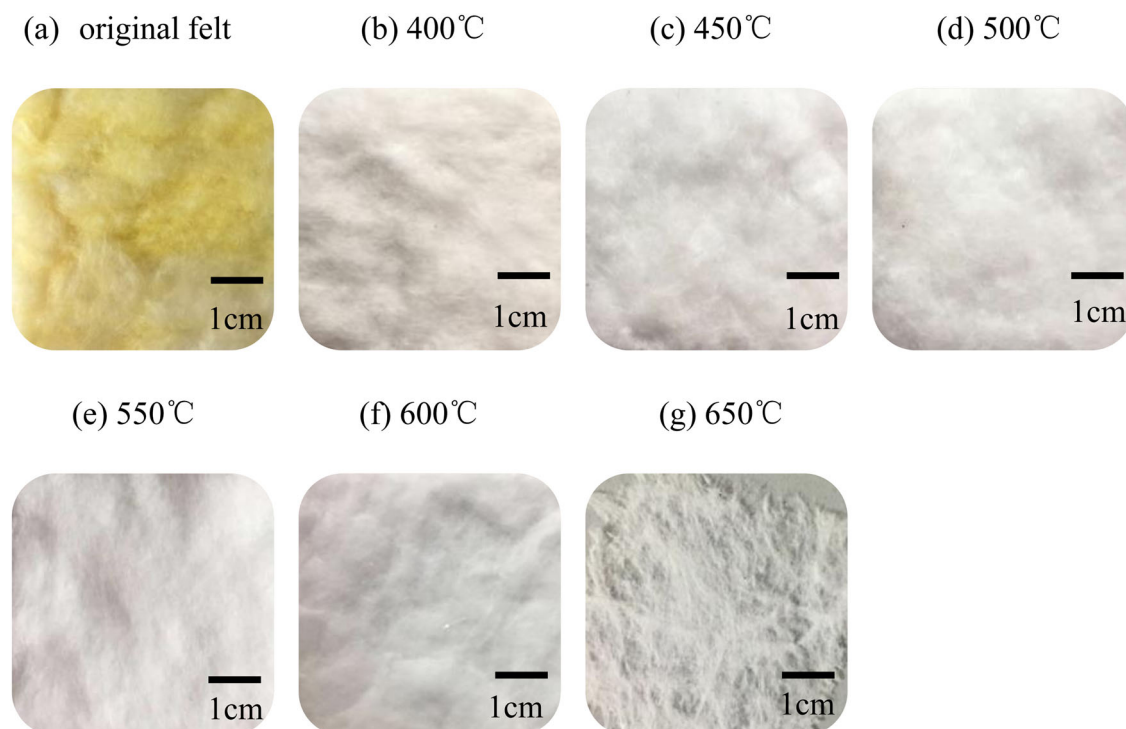


Figure 1. The surface optical images of original and heated superfine glass fiber felt.

et al., 2012), and some of them are used to absorb sound (Guangzhen et al., 2018), slight fog and insulate heat (S. Chen et al., 2018.). In recent years, normal glass fiber fabrics have been used on the steam piping as heat insulating material (Dai, 2017), but the superfine glass fibers are rarely used under high temperature. Up till now less research investigated the application of the superfine glass fiber under high temperature. Therefore, it is important to explore the external and internal characteristics of heated superfine glass fiber and develop its application at high temperature.

The purpose of the study is to investigate the influence of heat treatment on morphology, diameter and mesoporous of superfine glass fibers, as well as the corresponding mechanisms. The superfine glass fiber felt was heat-treated under a range of different temperatures of 400–650°C. The characteristics of the fiber morphology was investigated by SEM; the fiber diameter was studied by an inverted biologic microscope; the mesoporous and specific surface area were measured by following the method of Brunauer-Emmett-Teller (BET) with a Quantachrome QuadraSorb S1. In order to further explore the heat treatment mechanism, the internal characteristics and topographies of the fibers were analyzed by XRF, FTIR, XRD, TG and AFM. This research provides new insights into the external and internal characters of superfine glass fiber under high temperatures.

2. Experimental procedure and characterization

The superfine glass fiber has the following major chemical composition (%): 47 SiO₂, 26 Carbonate, 12 Na₂O, 7 CaO, 2 Al₂O₃, 2 MgO and others. The mean diameter of fiber was 2.27 μm. The aggregate of superfine glass fibers studied

herein was a superfine glass fiber felt. In the production process, fibers and the felt were formed almost at the same time. The degree of fiber damage could be deduced by the change in the appearance of the felt at high temperatures. In this paper, the superfine glass fiber felt was heat treated under 400°C, 450°C, 500°C, 550°C, and 600°C, 650°C, respectively, in air, using a ZSX1400 Muffle furnace (Cinite (Beijing) Technology Corp., Ltd). The heating temperature was started from room temperature to an ending temperature with a heating rate of 5°C/min, and then was maintained there for 30 min. No obvious difference in appearances of those heated felts were observed by naked eyes after heat treatments under 400–600°C, as shown in Figure 1. However, the superfine glass fibers piled together after the treatment under 650°C; and the fibers and felt were damaged and destroyed finally. Therefore, the fiber and felt treated under 400°C, 450°C, 500°C, 550°C and 600°C are discussed in the paper.

The diameter of fiber was measured using an inverted biologic microscope NIB-100, and was repeated 30 times to get a mean value. The morphology of the superfine glass fiber felt was observed with a scanning electron microscope (SEM, JSM-6390A, JEOL Ltd, Tokyo, Japan). The atomic force microscope (AFM, Bruker dimension, Germany) was used to examine the topography of fiber. The Fourier transform infrared (FTIR) spectrograms was tested by using a Spectrum Two FTIR spectrometer, Perkin Elmer (USA) in the range of 650–4000 cm⁻¹ with a resolution of 4 cm⁻¹. The X-ray fluorescence spectrometer (XRF) was tested by ZSX PrimusII, Rigaku (Japan). X-Ray diffraction (XRD) was performed on the original and heat-treated fibers using a wide-angle XRD instrument (Bruker D8 Advance, Germany) operated between 2θ = 10°–70°. Thermogravimetric analysis

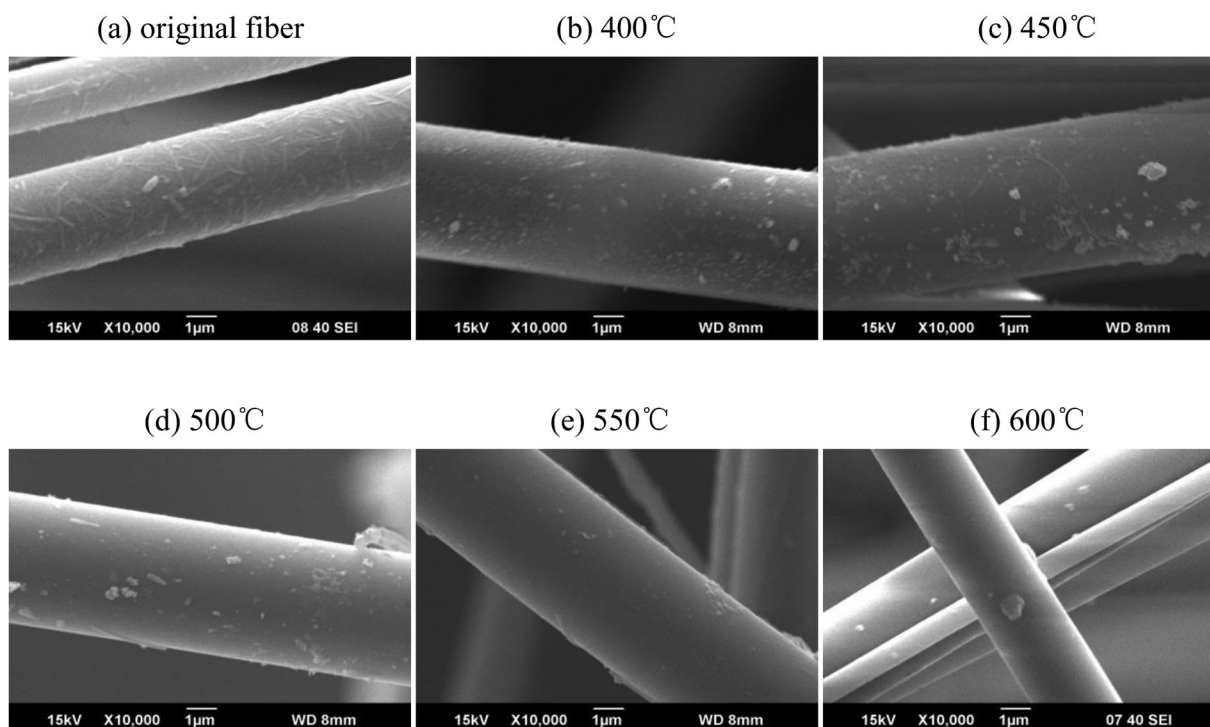


Figure 2. SEM morphologies of original and heated superfine glass fibers.

(TGA) of the fibers was performed in air and N_2 respectively at a heating rate of $10^\circ C/min$ using PerkinElmer STA8000 (American). The measurements of Brunauer-Emmett-Teller (BET) surface area, mesoporous size of superfine glass fiber were carried out using a Quantachrome QuadraSorb S1 with N_2 absorption, under a bath temperature of 77 K.

3. Results and discussion

3.1. Morphology of fibers

The surface morphology of the original fiber was coarse and in an uniformly distributed resinous matters, as shown in Figure 2a; while the surfaces of the heated fibers became smoother with the increasing temperature in Figure 2b–f; The uniformly distributed matters became spot-like substances spreading on the surface of the heated fibers. Normally, the resinous matter was sizing agents used in manufacturing the felt, and the spot-like substances were the residual sizing agents. At $600^\circ C$, the residual sizing agent almost all decomposed, making the most area of fiber surface smoothest; At this temperature, some heated fibers were cracked, as shown in Figure 2f.

In order to further investigate the morphological changes of the superfine glass fibers during the heat treatments, the topographies of fibers were tested by AFM, as shown in Figure 3. AFM images demonstrate that the surface of the fibers was coarse at $400^\circ C$, $450^\circ C$, $500^\circ C$, $550^\circ C$, but became smoother except with the granular protuberances at $600^\circ C$. The image Rq of the heated fiber increased with the temperature, increasing from $400^\circ C$ to $450^\circ C$, then decreased from $500^\circ C$ to $550^\circ C$. The Rq of the fiber heated

at $550^\circ C$ showed the lowest value of 1.96 nm; however, the Rq value of the fiber heated at $600^\circ C$ was the highest at 22.9 nm. Figure 3f demonstrated that most surface area of the $600^\circ C$ heated fiber was the smoothest and flat with a very smaller area of protruding spots, causing the image Rq was the highest than others. It can be deduced that the sizing agents on the surface of the heated fibers molten and piled together at 400 and $450^\circ C$, partly decomposed at $500^\circ C$ and $550^\circ C$. Finally, the residual sizing agents accumulated in very tiny areas on the surface of the heated fiber at $600^\circ C$. The corresponding process of the morphological changes of the fibers is shown in Figure 4.

3.2. Diameter of fibers

The mean diameter of the heated fibers increased by 7% when the temperature was heated to $400^\circ C$, then decreased significantly with the increasing temperature, as shown in Figure 5. The diameter came down to the original size at $450^\circ C$ and $500^\circ C$ and then further decreased by 6% and 14% under $550^\circ C$ and $600^\circ C$, respectively. The value of CV decreased with the heating temperature, except fluctuating at $500^\circ C$. The change of fiber diameter was mainly caused by the change of internal structure, which will be analyzed in Part 4 '4. Changes of structural characteristics of superfine glass fibers'.

3.3. Mesoporous and specific surface area of fibers

The mean mesoporous size of the original superfine glass fiber was 1.78 nm, then increased with the increasing temperature, except fluctuating at $500^\circ C$. The pore sizes of all

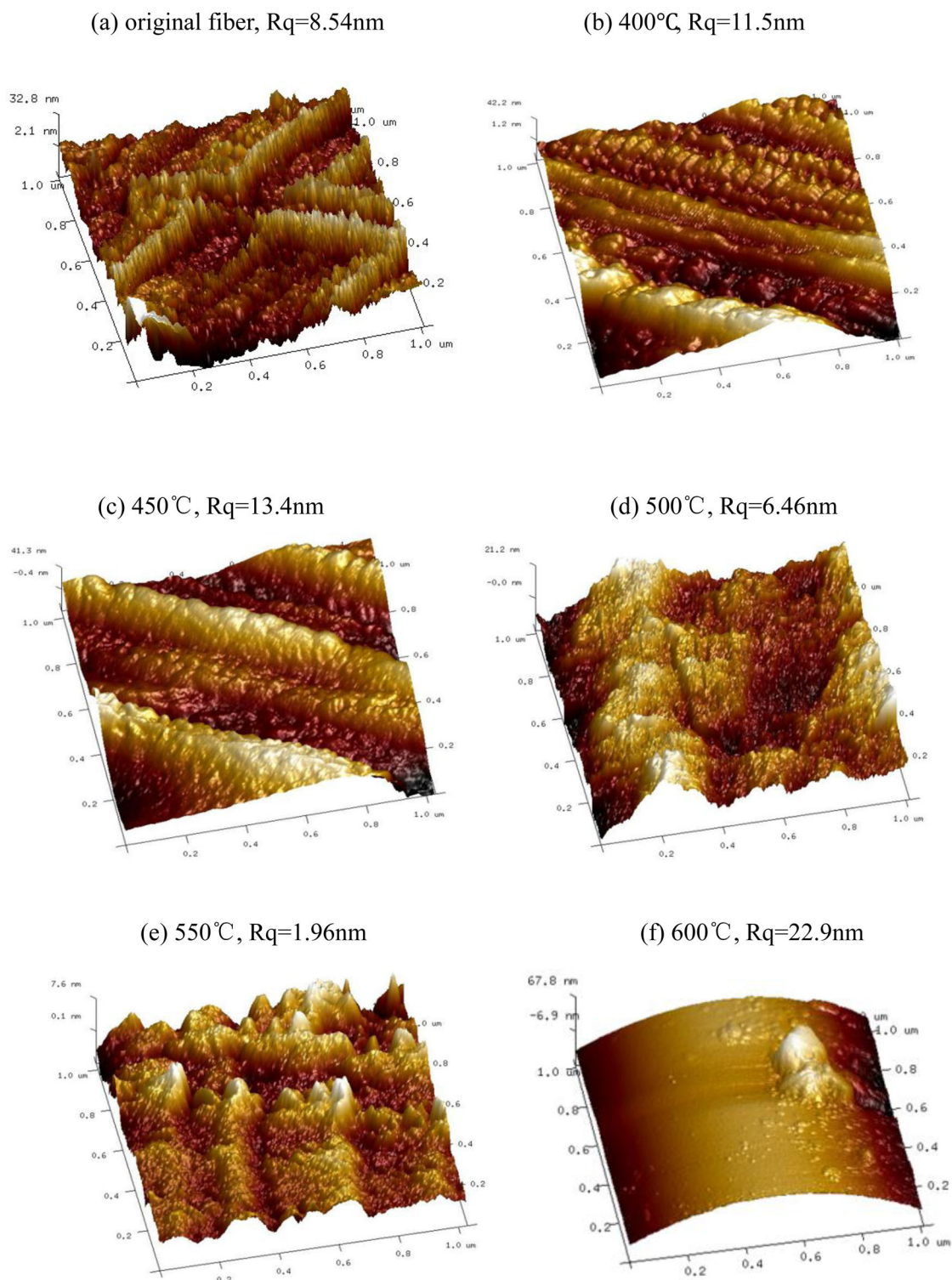


Figure 3. AFM and corresponding image Rq of original and heated superfine glass fibers.

heated fibers were higher than that of the original one, as shown in Figure 6. Corresponding to the mean mesoporous size, the MBET surface area of the original superfine glass fiber was $12.56 \text{ m}^2/\text{g}$, then decreased with increasing temperature, except fluctuated around 500°C . Also the MBET surface areas of all heated fibers were lower than that of the original one. The results reveal that the mean mesoporous size increased significantly, and the MBET surface

area decreased obviously. The MBET surface area decreased by 87.76% and the mean mesoporous size increased 5.13 times at 600°C compared to that of original one.

Figure 7 shows the relationship of the pore surface area and the numbers of mesoporous and mesoporous sizes of 3-50nm in the original and heated fibers. At the same mesoporous size, the higher pore surface area corresponded

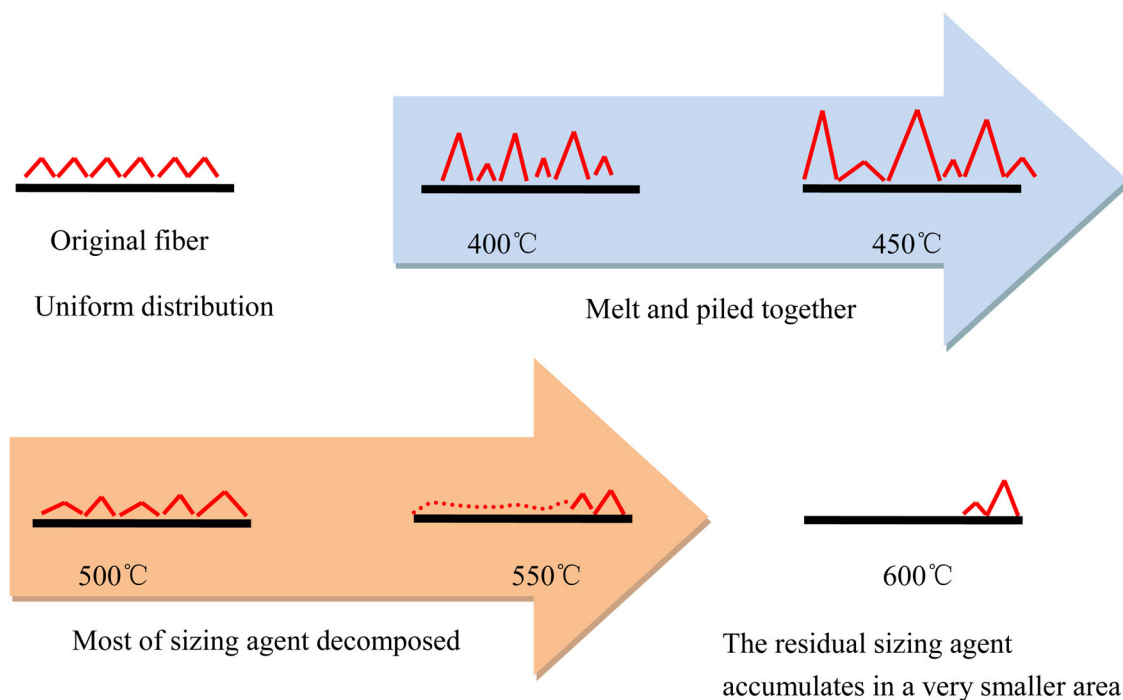


Figure 4. The heat treatments on surface characteristics of fibers.

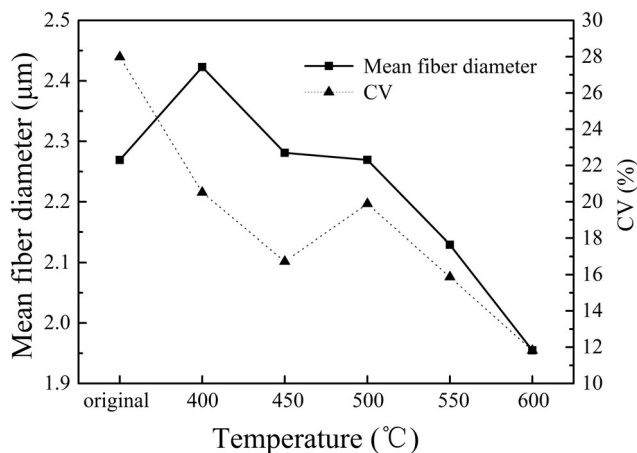


Figure 5. The mean diameter of original and heated superfine glass fibers.

with the more mesoporous. The number of pores in the heated fiber at 400 °C was the highest, then decreased with increasing temperature. The heated fibers showed the increased mesopores after heating under 400 – 550 °C, but the numbers was reduced at 600 °C than that of the original one.

4. Changes of structural characteristics of superfine glass fibers

In order to further explore the changes of fiber diameter, mesoporous and specific surface area of fibers, the internal structural characteristics of superfine glass fibers were tested and analyzed. Firstly, the FTIR spectra of the original and heated fibers were compared and shown in Figure 8. The vibrational band at 1726 cm⁻¹ was due to deformation vibrations of adsorbed water molecules (Hoang et al., 2010; Tenorio et al., 2018). The bands nearby 833.88, 974.56, and

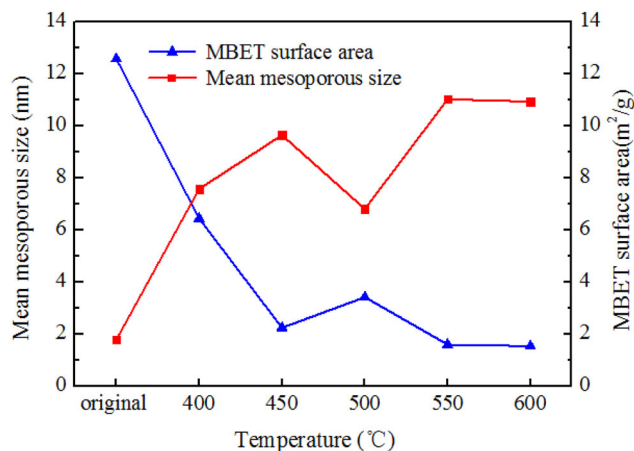


Figure 6. MBET surface areas and mean mesoporous sizes of original and heated superfine glass fibers.

1451.3 cm, were ascribed to the asymmetric and symmetric Si–O stretching vibration and Si–O–Si bending vibrations respectively (Hao & Yu, 2009a; Salunkhe et al., 2018). The strong and sharp bands were silicon oxide SiO₂ confirming the chemical structure of the fibers. The spectra of the original fiber exhibited the strong and sharp bands at 974.56 cm⁻¹, with transmittance 88%, while decreased to 75% after the fiber being treated at 600 °C. It meant that more SiO₂ were transferred at 600 °C, and the content of SiO₂ was increased.

At 600 °C, the absorption bands of the fibers shifted from the original 974.56, 1451.3, 1726.7, 3400 cm⁻¹ to 954.94, 1253.5, 1649.1, and 3372.32 cm⁻¹, respectively. These shifts in band positions might be attributed to the changes of conformation geometry of fibers (Saikia et al., 2006.), indicating that the conformation geometry changed obviously at 600 °C.

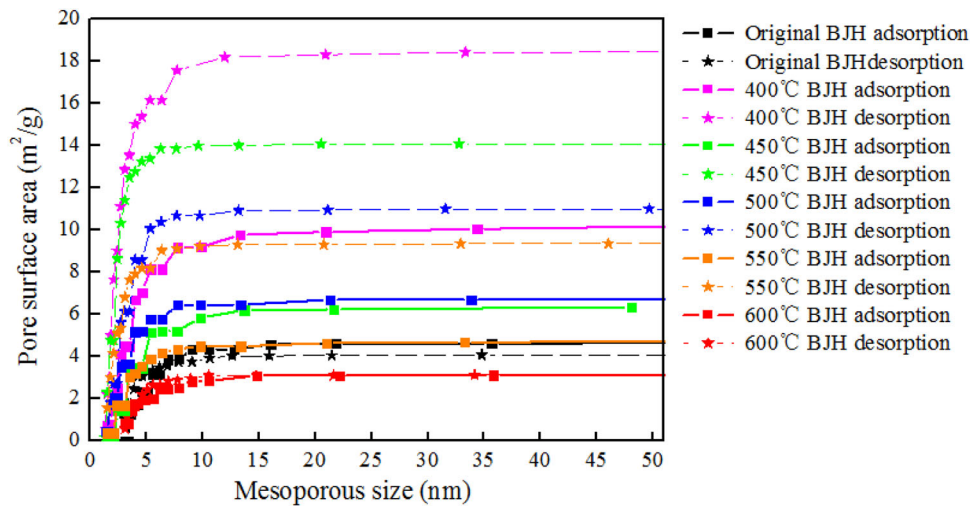


Figure 7. Pore surface area distribution of original and heated superfine glass fibers.

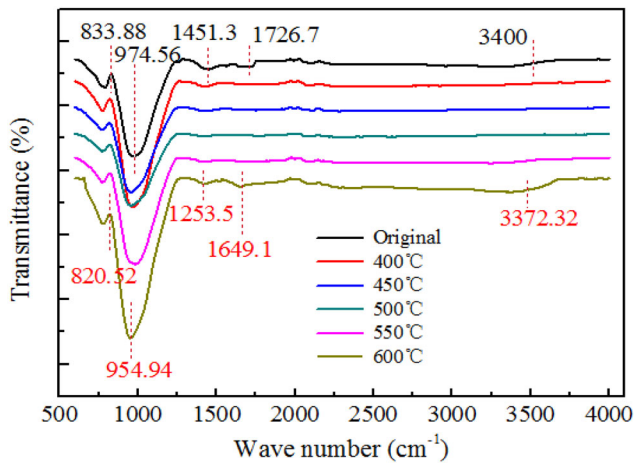


Figure 8. FTIR of original and heated superfine glass fibers.

The mass percentage of carbonate (CO_3^{2-}) decreased significantly during the heat treatments, as shown in Figure 9a. A 88% decrease was found for the fibers heated at 600 °C; however, the mass percentage of SiO_2 increased obviously, and increased about 24% at 600, which was confirmed by FTIR. In general, silicate compounds were extremely stable below 600 °C, while some carbonate compounds were more vulnerable to decompose.

The mass percentages of many metal oxides changed obviously during the heat treatments. The mass percentages of Na_2O , CaO , Al_2O_3 , MgO , K_2O , Fe_2O_3 increased, ZnO and BaO fluctuated obviously, TiO_2 and SrO kept stable, as shown in Figure 9. During the heat treatments, some divalent cations (such as Mg^{2+}) diffused from the interior to the surface where they could react with environmental oxygen and formed corresponding metal oxides (MgO) (Fiore et al., 2015). It can be deduced that the some carbonates broke down into metal oxide and CO_2 during the heat treatments. Normally some carbonates broke down below 600 °C such as MgCO_3 and ZnCO_3 ; some broke down above 600 °C such as BaCO_3 and SrCO_3 ; and some partly decomposed near by 600 °C, such as CaCO_3 ; and some could melt, including K_2CO_3 and Na_2CO_3 . As Figure 7 showed, the heated fibers had more mesopores formed during heating

under 400 – 550 °C, but less was formed at 600 °C than the original one. Therefore, it could be speculated that most carbonates thermally decomposed under 400 – 550 °C, making the number of mesopores increased; then the thermal melting of the fibers intensified above 550 °C, causing the number of mesopores decreased at 600 °C.

The thermal decomposition of the fibers was investigated by thermo-gravimetric analysis (TGA), as presented in Figure 10. For the original fiber, the weight loss nearby 100 °C was ascribed to the vaporization of surface water (Hao & Yu, 2009b), consistent with the results of FTIR. The weight loss of the original fiber was very fast and significant in the stage 100–550 °C, but unchanged above ~ 600 °C. The fibers heated under 400 °C, 450 °C, 500 °C, and 550 °C had a similar trend of TG curves with an obvious weight gain phenomenon. The TG curve of the fiber heated at 400 °C showed the residual weight of the fiber increased firstly, decreased in the stage of 200 – 400 °C, then increased during 400 – 800 °C. TG curves of all heated fibers under 450 °C and 500 °C presented the increase in the residual weights. And the weights of the fibers rose with the heating temperature. The fiber treated under 500 °C presented the highest increase in the TG curve, corresponding with the highest residual weight. But the residual weight of the fiber heated under 550 °C initially dropped and then increased. The TG curve of fiber heated under 600 °C fluctuated slightly and the residual weight was 99% of the original weight.

With the observation of morphological changes of the fibers heated under the same temperatures ranges, the weight changes might be related to the changes of chemical compositions as demonstrated in Figure 9. When carbonates were decomposed in the heated fibers, the metal oxides stayed in the heated fibers and some metal ions, such as Mg ions, might diffuse out to surfaces of the heated fiber from inside in reduced status (Mg). The diffusion process was incomplete under temperature range of 400–550 °C but might be complete under 600 °C. When the metal ions (Mg) was further heated with the existence of oxygen, it may form metal oxide (MgO) gaining weight. Then we removed the environmental oxygen, which means that the TGA was tested in N_2 , without O_2 , as shown in Figure 11. Obviously, there was no obviously weight gain phenomenon.

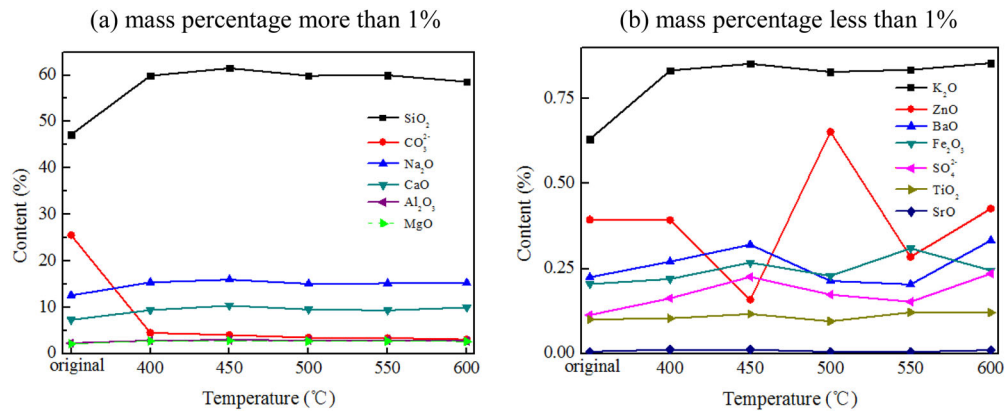


Figure 9. The mass percentage of original and heated superfine glass fibers (%).

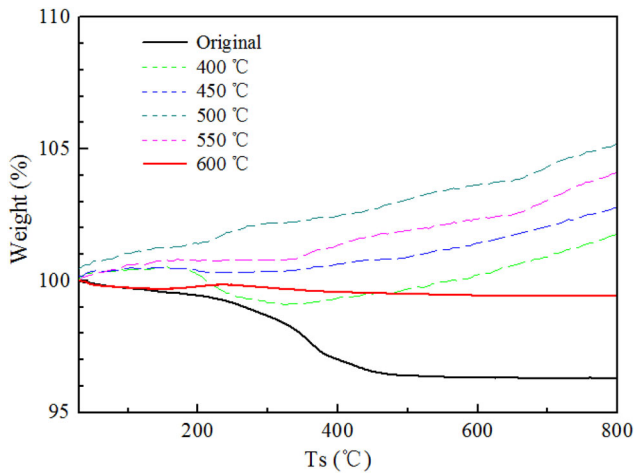


Figure 10. TG curves of original and heated superfine glass fibers under air atmosphere.

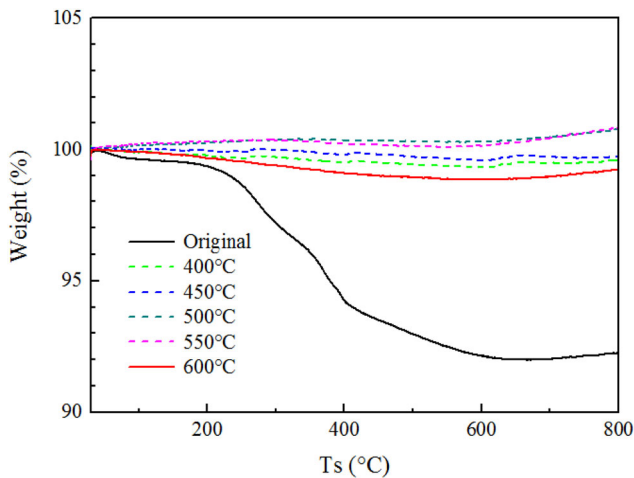


Figure 11. TG curves of original and heated superfine glass fibers under N_2 .

On the other hand, a proposed additive theory (Z. F. Chen, 2016) showed the properties of glass varied with the mass fraction. The general properties were determined by the sum of the single properties of oxides contained in the glass. For example, the volume of glass increased with the increasing content of K_2O . As XRF analysis showed the content of melt oxide changed obviously after heat treatment. Hence, the additive property of heated fiber was influenced, which

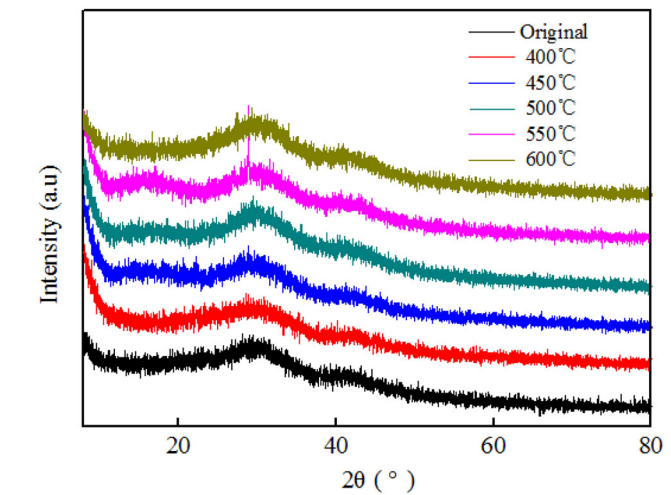


Figure 12. X-ray diffraction spectra of original and heated superfine glass fibers.

Table 1. Crystallinity of original and heated superfine glass fibers.

	Original	400 °C	450 °C	500 °C	550 °C	600 °C
Crystallinity / %	19.97	10.41	7.93	14.57	18.96	21.38
Difference / %	-	-47.87	-60.29	-27.04	-5.06	+7.06

finally caused the weight gain phenomenon. Based on the above analysis, it could be deduced that most carbonates were decomposed into metal oxides and CO_2 during heat treatment.

There were no significant difference between the XRD spectra of the original and heated fibers, as shown in Figure 12. The diffraction peak nearby $2\theta = 30^\circ$ was a characteristic peak of amorphous SiO_2 (Qiu et al., 2018). Table 1 showed the crystallinity of heated fiber significantly decreased from 400 °C to 450 °C, then increased with increasing heating temperature. The crystallinity of the fiber heated at 600 °C was 21.38%, increased by 7.06% versus the original one. Those results indicate that the more crystals may be formed from heated fiber at 600 °C.

The FTIR stated the absorption bands shifted, and the conformation geometry of molecule changed after high-temperature treatment. The carbonate broken down, then the CO_2 produced and moved. Those caused the superfine glass fiber was in a metastable state for a long time and

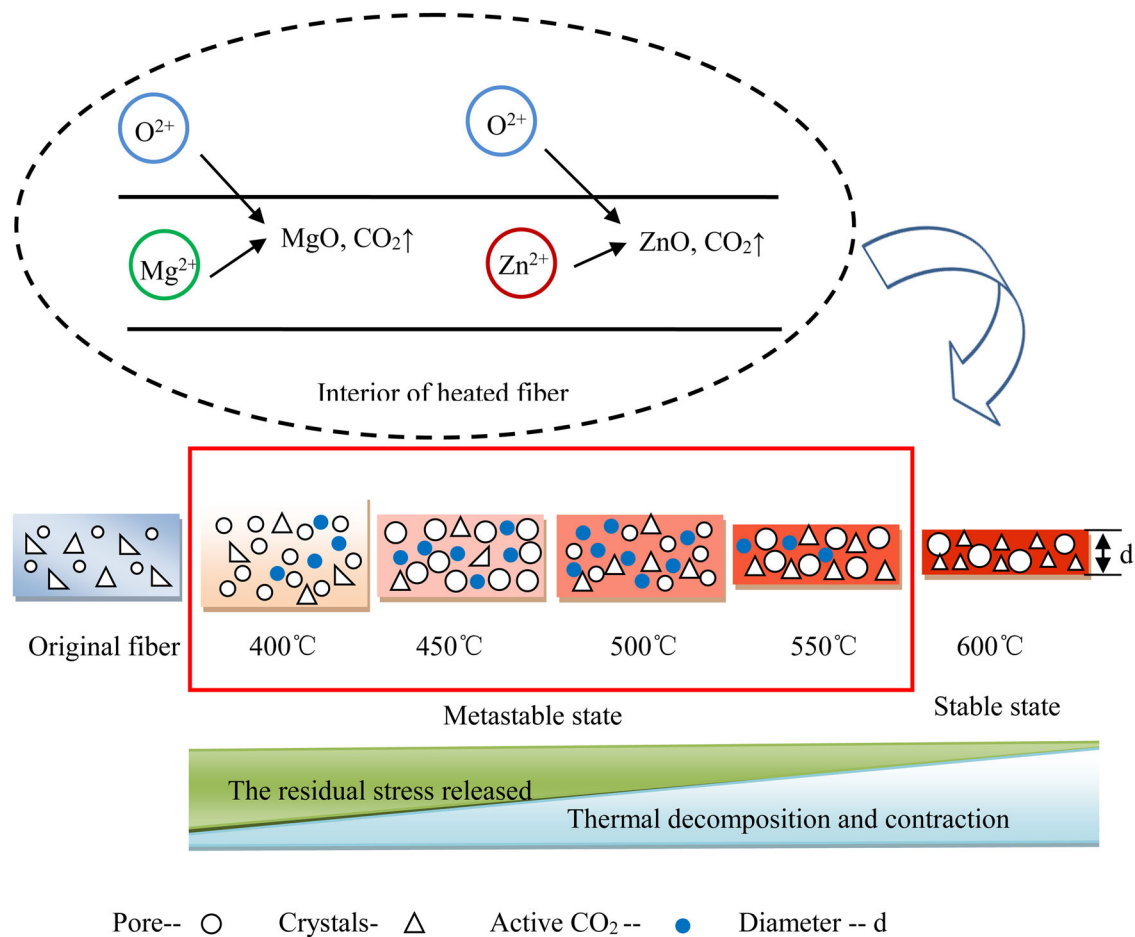


Figure 13. Structural changes of superfine glass fibers during heat treatment.

contained excess internal energy. Under the heat action of the test process, it was possible to convert to low energy. It meant that the crystallization was possible. And these finally resulted in the change of mesoporous distribution and external fiber diameter during heat treatment.

Additionally, the superfine glass fiber was produced by drawing and cooling. Therefore there was a large amount of residual stress in the glass fiber (Ye & Chen, 2017). During heat treatment, an ‘annealing effect’ was formed. The residual stress was gradually released, which made the fiber shrunk or contracted. Finally, the length of the fibers decreased, and the diameter increased. In this paper, not only the surface residual stress but also the decomposition and melting of carbonate were found affecting the diameter of the heated fibers. At 400 °C, the residual stress released in main, which caused the diameter of heated fiber increased; while above 450 °C, the carbonate decomposed and melted, which became the main factor causing the diameter decreased with increasing temperature. The structural change process of the fibers is presented in Figure 13.

5. Conclusions

In this article, the effect of heat treatment on the properties of superfine glass fiber are discussed by treating the superfine glass fiber felt under varied high temperatures of 400 °C, 450 °C, 500 °C, 550 °C, 600 °C, 650 °C, respectively.

The fibers treated below 600 °C were studied since 650 °C destroyed the felt. During the heat treatments, sizing agents on the surface of the fibers gradually melt and decompose with the increasing temperature. The residual sizing agents gradually accumulate on surfaces of the fibers forming smaller spot. The fibers heated under 550 °C possessed the lowest image Rq 1.96 nm; however, under 600 °C, the fibers showed the highest image Rq of 22.9 nm, with most surface area, the smoothest among others.

During heat treatments, the carbonate break down to metal oxide and CO₂, some crystals formed, and the molecule geometry conformation changed, making the heated fibers stay in a metastable state at the temperature of 400 °C, 450 °C, 500 °C, 550 °C and in a more stable state at 600 °C. The obviously weight gain phenomenon occurs in the heated fiber at 400 °C, 450 °C, 500 °C and 550 °C, a reflection of such structural change. The residual stress released in fibers, the decomposition and melting of carbonate eventually increased the diameter of heated fiber at 400 °C and then decreased with the increasing temperature. The mesoporous size of the heated fibers increased, and the specific surface area decreased significantly. The number of mesopores increased heating under 400 °C obviously, then decreased with increasing temperature.

Comparing the fibers heated under 600 °C with the original one, the former has mass percentage of carbonates decreased by 88% and SiO₂ increased by 24%, crystallinity

increased by 7.06% in the structures. Meanwhile, the diameter of the fiber heated under 600 °C decreased by 14%; the mean mesoporous size increased 5.13 times, while the number of mesopores decreased; the specific surface area decreases by 87.76%.

Disclosure statement

No potential conflict of interest was reported by the author(s).

Funding

This work was financially supported by National Key R&D Program of China (Project No. 2018YFC2000900), the Fundamental Research Funds for the Central Universities (Project No. CUSF-DH-D-2018020) and (Project No. 2232018A3-04).

References

- Abbasi, A., & Hogg, P. J. (2005). Temperature and environmental effects on glass fibre rebar: Modulus, strength and interfacial bond strength with concrete. *Composites Part B: Engineering*, 36(5), 394–404. <https://doi.org/10.1016/j.compositesb.2005.01.006>
- Bal, B. C., Bektaş, İ., Mengeloğlu, F., Karakuş, K., & Ökkeş Demir, H. (2015). Some technological properties of poplar plywood panels reinforced with glass fiber fabric. *Construction and Building Materials*, 101, 952–957. <https://doi.org/10.1016/j.conbuildmat.2015.10.152>
- Chen, S., Xiao, D., & Liu, M. (2018). China patent no. CN207863796-U.
- Chen, Z. F. (2016). *Wuji feijinshu cailiaoxue* (Vol. 2). Northwestern Polytechnical University Press. (in Chinese).
- Chen, H., Wang, J., Ni, A., Ding, A., Sun, Z., & Han, X. (2018). Effect of novel intumescent flame retardant on mechanical and flame retardant properties of continuous glass fibre reinforced polypropylene composites. *Composite Structures*, 203, 894–902. <https://doi.org/10.1016/j.compstruct.2018.07.071>
- Chen, Z. F., Wu, C., Yang, Y., Li, B. B., Chen, Z., Qiu, J. L., & Su, D. (2016). Preparation of super-fine aviation glass wool and its property study on sound and thermal insulation. *Journal of Nanjing University of Aeronautics & Astronautics*, 48(1), 10–15. (in Chinese).
- Dai, G. (2017). China Patent No. CN107143727-A, CN207246665-U.
- Elbadry, E. A., Abdalla, G. A., Aboaraia, M., & Oraby, E. A. (2017). Notch sensitivity of short and 2D plain woven glass fibres reinforced with different polymer matrix composites. *Journal of Reinforced Plastics and Composites*, 36(15), 1092–1098. <https://doi.org/10.1177/0731684417702529>
- Feih, S., Manatpon, K., Mathys, Z., Gibson, A. G., & Mouritz, A. P. (2009). Strength degradation of glass fibers at high temperatures. *Journal of Materials Science*, 44(2), 392–400. <https://doi.org/10.1007/s10853-008-3140-x>
- Fiore, V., Scalici, T., Di Bella, G., & Valenza, A. (2015). A review on basalt fibre and its composites. *Composites Part B Engineering*, 74, 74–94. <https://doi.org/10.1016/j.compositesb.2014.12.034>
- Gao, S. L., Mäder, E., & Plonka, R. (2007). Nanostructured coatings of glass fibers: Improvement of alkali resistance and mechanical properties. *Acta Materialia*, 55(3), 1043–1052. <https://doi.org/10.1016/j.actamat.2006.09.020>
- Guangzhen, L., Li, Q., & Zhanchao, Z. (2018). China Patent No. CN206929141-U.
- Hao, L. C., & Yu, W. D. (2009a). Comparison of the morphological structure and thermal properties of basalt fiber and glass fiber. *Journal of Xi'an Polytechnic University*, 23(2), 327–332. [https://doi.org/10.13338/j.issn.1674\(inChinese\)](https://doi.org/10.13338/j.issn.1674(inChinese))
- Hao, L. C., & Yu, W. D. (2009b). Evaluation of thermal protective performance of basalt fiber nonwoven fabrics. *Journal of Thermal Analysis and Calorimetry*, 100(2), 551–555. <https://doi.org/10.1007/s10973-009-0179-0>
- Hoang, V. D., Dang, T. P., Dinh, Q. K., Nguyen, H. P., & Vu, A. T. (2010). The synthesis of novel hybrid thiol-functionalized nanostructured SBA-15. *Advances in Natural Sciences: Nanoscience and Nanotechnology*, 1(3), 035011. <https://doi.org/10.1088/2043-6262/1/3/035011>
- Katz, A., & Berman, N. (2000). Modeling the effect of high temperature on the bond of FRP reinforcing bars to concrete. *Cement and Concrete Composites*, 22(6), 433–443. [https://doi.org/10.1016/S0958-9465\(00\)00043-3](https://doi.org/10.1016/S0958-9465(00)00043-3)
- Minty, R. F., Yang, L., & Thomason, J. L. (2018). The influence of hardener-to-epoxy ratio on the interfacial strength in glass fibre reinforced epoxy composites. *Composites Part A Applied Science and Manufacturing*, 112, 64–70. <https://doi.org/10.1016/j.compositesa.2018.05.033>
- Prusty, R. K., Rathore, D. K., & Ray, B. C. (2018). Water-induced degradations in MWCNT embedded glass fiber/epoxy composites: An emphasis on aging temperature. *Journal of Applied Polymer Science*, 135(11), 45987. <https://doi.org/10.1002/app.45987>
- Qiu, B., Li, K., & Li, X. (2018). Synthesis and enhanced luminescent properties of SiO₂@LaPO₄:Ce³⁺/Tb³⁺ microspheres. *Optical Materials Express*, 8(1), 59–65. <https://doi.org/10.1364/OME.8.000059>
- Raju, B. R., Suresha, B., Swamy, R. P., & Kanthraju, B. S. G. (2013). Investigations on mechanical and tribological behaviour of particulate filled glass fabric reinforced epoxy composites. *Journal of Minerals and Materials Characterization and Engineering*, 1(4), 160–167. <https://doi.org/10.4236/jmmce.2013.14027>
- Saikia, L., Srinivas, D., & Ratnasamy, P. (2006). Chemo-, regio- and stereo-selective aerial oxidation of limonene to the endo-1,2-epoxide over Mn(Salen)-sulfonated SBA-15. *Applied Catalysis A: General*, 309(1), 144–154. <https://doi.org/10.1016/j.apcata.2006.05.011>
- Salunkhe, N. G., Ladole, C. A., Thakare, N. V., & Aswar, A. S. (2018). MgFe₂O₄@SiO₂-SO₃H: An efficient, reusable catalyst for the microwave-assisted synthesis of benzoxazinone and benzthioxazinone via multicomponent reaction under solvent free condition. *Research on Chemical Intermediates*, 44(1), 355–372. <https://doi.org/10.1007/s11164-017-3108-z>
- Sever, K., Sarikanat, M., Seki, Y., Cecen, V., & Tavman, I. H. (2008). Effects of fiber surface treatments on mechanical properties of epoxy composites reinforced with glass fabric. *Journal of Materials Science*, 43(13), 4666–4672. <https://doi.org/10.1007/s10853-008-2679-x>
- Shayed, M. A., Cherif, C., Hund, R. D., Cheng, T., & Osterod, F. (2010). Carbon and glass fibers modified by polysilazane based thermal resistant coating. *Textile Research Journal*, 80(11), 1118–1128. <https://doi.org/10.1177/0040517509357648>
- Spagnuolo, S., Meda, A., Rinaldi, Z., & Nanni, A. (2018). Residual behaviour of glass FRP bars subjected to high temperatures. *Composite Structures*, 203, 886–893. <https://doi.org/10.1016/j.compstruct.2018.07.077>
- Tenorio, M. J., Morère, J., Carnerero, C., Torralvo, M. J., Pando, C., & Cabañas, A. (2018). Thiol group functionalization of mesoporous SiO₂ SBA-15 using supercritical CO₂. *Microporous and Mesoporous Materials*, 256, 147–154. <https://doi.org/10.1016/j.micromeso.2017.07.056>
- Wang, Y. H., Qi, G. H., Lu, Y. B., Cui, S. L., & Jiang, S. J. (2012). Use of superfine glass fiber in composite filter media. *Fiber Glass*, 2012(1), 37–39. <https://doi.org/10.13354/j.cnki.cn32-1129/tq.2012.01.010> (in Chinese).
- Ye, X. L., & Chen, Z. F. (2017). Properties of ultrafine glass wool felt after high-temperature treatment. *Journal of Nanjing University of Aeronautics & Astronautics*, 49(4), 580–585 (in Chinese).
- Younes, A., Sankaran, V., Seidel, A., & Cherif, C. (2014). Study of tensile behavior for high-performance fiber materials under high-temperature loads. *Textile Research Journal*, 84(17), 1867–1880. <https://doi.org/10.1177/0040517513499434>